Vallee, B. L., and Wacker, W. E. C. (1970), *Proteins 2nd Ed. 5.*
Vallee, B. L., and Williams, R. J. P. (1968a), *Proc. Natl. Acad. Sci. U.S.A. 59,* 498–505.
Vallee, B. L., and Williams, R. J. P. (1968b), *Chem. Br. 4,* 397–402.
Wilson, I. B., Dayan, J., and Cyr, K. (1964), *J. Biol. Chem. 239,* 4182–4185.
Wood, D. L., and Remeika, J. P. (1967), *J. Chem. Phys. 46,* 3595–3602.

Molecular Asymmetry in an Abortive Ternary Complex of Lobster Glyceraldehyde-3-phosphate Dehydrogenase†

R. Michael Garavito,‡ Denis Berger,§ and Michael G. Rossmann*

ABSTRACT: An abortive ternary complex of lobster glyceraldehyde-3-phosphate dehydrogenase was produced by the covalent attachment of 3,3,3-trifluoroacetone to Cys-149 in each subunit. X-ray diffraction analysis of the glyceraldehyde-3-phosphate dehydrogenase–trifluoroacetone–nicotinamide adenine dinucleotide complex showed asymmetry with respect to the active-site conformations of the trifluoroacetone substrate analogue and some catalytic groups. These results are consistent with ^{19}F nuclear magnetic resonance observations of this complex (Bode, J., Blumenstein, M., and Raftery, M. A. (1975), *Biochemistry 14,* 1153–1160). Different substrate conformations were found on opposite sides of the molecular diad relating subunits whose active centers are in close proximity (the *R* axis).

The interaction of D-glyceraldehyde-3-phosphate dehydrogenase (EC 1.2.1.12) with a variety of ligands is frequently different within each subunit. For instance, the apo–holo enzyme transition can exhibit either negative (Conway and Koshland, 1968; De Vijlder et al., 1969; Boers and Slater, 1973; Schlessinger and Levitzki, 1974) or positive (Cook and Koshland, 1970; Kirschner, 1971; Kirschner et al., 1971) cooperativity, and the covalent addition of substrate analogues to only two of the subunits can completely inactivate the enzyme (MacQuarrie and Bernhard, 1971; Stallcup and Koshland, 1973; Levitzki, 1973; Seydoux et al., 1973; Bernhard and MacQuarrie, 1973). On the other hand, the binding of NAD^+ to acylated enzyme (Seydoux et al., 1976) and the formation of the Racker band (Racker and Krimsky, 1952; Krimsky and Racker, 1955) is apparently identical in all subunits. The two models (Figure 1) which have been proposed to explain the functional nonequivalence of active sites in terms of conformational asymmetry are based on either ligand-induced conformational transitions (Stallcup and Koshland, 1973; Levitzki, 1973) or preexisting molecular asymmetry (Bernhard and MacQuarrie, 1973).

Conformational asymmetry has been observed for oligomeric proteins in insulin (Blundell et al., 1972; Hodgkin, 1974; Bentley et al., 1976), α-chymotrypsin dimers (Tulinsky et al., 1973), and tobacco mosaic virus (Champness et al., 1976). Asymmetry in the binding affinity of ligands to covalently identical subunits has been shown for NAD^+ to soluble malate dehydrogenase (Hill et al., 1972) and for sugars to hexokinase (Anderson and Steitz, 1975). Conformational asymmetry has been induced on binding of coenzyme to lactate dehydrogenase (Adams et al., 1970) and removal of calcium from concanavalin A (Jack et al., 1971).

Crystals of human holo-GAPDH[1] (Watson et al., 1972; Mercer et al., 1976) show a crystallographic twofold axis coincident with the *Q* molecular axis (see Buehner et al. (1974a) for the nomenclature of the three orthogonal *P, Q, R* molecular axes). The three-dimensional structure of lobster holo-GAPDH exhibits 222 symmetry to within the accuracy of a 3.0-Å resolution electron-density map (Buehner et al., 1974a). Moras et al. (1975) subsequently showed that a more accurate map at 2.9-Å resolution suggested asymmetry of the protein structure between active centers as well as asymmetry of bound NAD^+. Their results indicate a conservation of the *Q* axis but not of the *P* and *R* axes, consistent with the observations on human holo-GAPDH and the anticipated cooperative interaction of the subunits across the *R* axis (Buehner et al., 1974a). Nevertheless, the validity of these conclusions was brought into question by observing symmetric binding of nicotinamide 8-bromoadenosine dinucleotide to lobster GAPDH (Olsen et al., 1976a) and symmetric displacement of sulfate by citrate ions from the active center (Olsen et al., 1976b).

Bode et al. (1975a,b) studied the interaction of the substrate analogue 3,3,3-trifluorobromoacetone with rabbit muscle GAPDH. The TFA label was of the approximate size and shape as the natural thioester intermediate (Figure 2) which, it was hoped, would mimic the true enzyme–substrate complex, although McCaul and Byers (1976) have shown that analogues without a terminal phosphate have decreased reactivity. The CF_3 group acted as a probe in the subsequent ^{19}F nuclear magnetic resonance study of Bode et al. (1975a). They observed both the reduction of the keto group by NADH and

† From the Department of Biological Sciences, Purdue University, West Lafayette, Indiana 47907. *Received April 8, 1977.* The work was supported by the National Institutes of Health (Grant GM 10704) and the National Science Foundation (Grant BMS74-23537).
‡ Supported by a National Institutes of Health Molecular and Cellular Biology Training Grant.
§ Supported by a postdoctoral fellowship from the Swiss National Science Foundation. Present address: Hopital Contonal, Institut Universitaire de Medicine Physique et de Reeducation, 1211 Geneve 4, Switzerland.

[1] Abbreviations used are: GAPDH, D-glyceraldehyde-3-phosphate dehydrogenase; TFA-Br, trifluorobromoacetone; TFA, trifluoroacetonyl; PGA, 3-phosphoglycerate; NAD^+, nicotinamide adenine dinucleotide; NADH, reduced NAD^+; EDTA, (ethylenedinitrilo)tetraacetic acid.

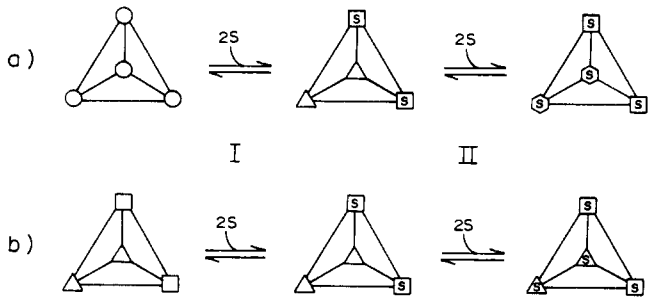

FIGURE 1: Representation of (a) the ligand-induced asymmetry model (Stallcup and Koshland, 1973) and (b) the preexisting asymmetry model (Bernhard and MacQuarrie, 1973). This figure has been adapted from Figure 9 in the paper by Stallcup and Koshland (1973). The fast step is indicated by I and the subsequent slow step by II.

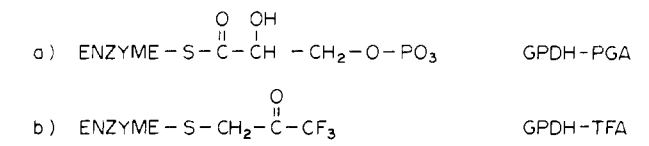

FIGURE 2: Schematic diagram showing the similarity between (a) the natural acyl intermediate GAPDH-PGA and (b) the GAPDH-TFA alkylated complex.

biphasic kinetics for the covalent attachment of the TFA analogue to the essential thiol (Bode et al., 1975b). Two distinct fluorine environments were found within the GAPDH-TFA complex (Bode et al., 1975a). This asymmetry was absent below pH 6.5 and reached a maximum at around pH 8.2 in the presence of coenzyme, although the asymmetry lost its pH dependence when the NAD^+ was replaced by pyridine-3-aldehyde AD^+. They concluded that the GAPDH-TFA·NAD^+ complex was asymmetric and affected the conformation of the TFA label within the active center, in support of Bernhard's hypothesis (Figure 1).

Reported here is an investigation of the crystalline GAPDH-TFA·NAD^+ abortive ternary complex by x-ray diffraction methods in an attempt to explore further the substrate binding and structural basis of the asymmetric behavior of the GAPDH molecule. This work has close similarity to the studies of alkylated intermediates of the cysteine protease papain (Drenth et al., 1976) and of the serine proteases subtilisin BPN′ (Robertus et al., 1972) and γ-chymotrypsin (Segal et al., 1971).

Materials and Methods

The enzyme was prepared using the procedure described by Buehner et al. (1974b) and had specific activity and NAD^+ content comparable to that reported by Allison (1966) and Boers et al. (1971). NAD^+ was obtained from P-L Biochemicals and 3,3,3-trifluorobromoacetone was purchased from Peninsular Chemresearch, Inc.

The alkylation of GAPDH, by elimination of HBr from TFA-Br and GAPDH, was done under essentially identical conditions as described by Bode et al. (1975b). A solution of 0.01 M ethylenediamine chloride, 0.1 M KCl, 1 mM EDTA, 0.5 mM NAD^+, and 5 mg/mL enzyme (at pH 7.0) was prepared. The TFA-Br was added until a concentration of 5 mM was reached, thus initiating the reaction. This reaction mixture was incubated for 2 h at 4 °C, and then centrifuged for 20 min at 10 000*g* to remove any precipitate. The mixture was subsequently dialyzed overnight against 50% ammonium sulfate, 1 mM EDTA, 1 mM dithiothreitol, and 0.5 mM NAD^+ (pH 6.2), and the enzyme was precipitated by addition of ammonium sulfate (solid or saturated solution). The precipitate was collected by centrifugation at 10 000*g* for 30 min, and dissolved in a minimal amount of distilled water. This enzyme solution was dialyzed against 50% ammonium sulfate, 1 mM EDTA, 0.5 mM NAD^+ (pH 8.0) overnight. The enzyme solution was adjusted to a protein concentration of between 14 and 16 mg/mL, assuming that the extinction coefficient at 280 nm for the GAPDH-TFA·NAD complex is the same as for the holoenzyme, 0.98 optical density unit mg^{-1} mL^{-1}. The ternary complex was crystallized from this enzyme solution by the vapor-diffusion method with 72% ammonium sulfate at pH 8.0 in the diffusion reservoir.

The ternary complex under the above conditions crystallizes in two crystal forms. The first one consists of long prismatic crystals of space group $P2_1$ with cell parameters a = 151.3 Å, b = 96.4 Å, c = 134.7 Å, β = 111° 30′ and with apparently two tetramers per asymmetric unit. Though these crystals diffract to high resolution, they shatter and dissolve within 3 weeks of formation. The second crystal form is isomorphous with the orthorhombic holoenzyme form (Watson and Banaszak, 1964), and was used to collect 2.9-Å resolution x-ray diffraction data according to the precession camera data-collection scheme described by Buehner et al. (1974b). Twenty-three x-ray diffraction photographs were taken and processed, providing 21 051 independent reflections (33 302 independent reflections were observed for the native holoenzyme structure on 53 films). Agreement between structure amplitudes measured on different films was 5.5%, comparable to the results for the native data (Buehner et al., 1974a). The selected photographs covered the complete 6.0-Å resolution sphere and sampled the reciprocal lattice as evenly as possible to higher resolution. The root mean square difference between the TFA and native data was about 10% of mean F. About 59% of the data was present in the range from 6.0- to 2.9-Å resolution. A difference electron-density map was computed using ($F_{TFA} - F_{holo}$) Fourier coefficients and the holoenzyme double isomorphous replacement phases (Moras et al., 1975). In the absence of a refined structure, due to the lack of available data beyond 2.9-Å resolution, the isomorphous replacement phases were preferred over calculated phases. The resulting difference electron-density map in crystallographic space was transformed into a map using the three available molecular diads, P, Q, and R, as coordinate axes (see Buehner et al., 1974b).

Results

The largest peaks on the difference electron-density map were at the heavy-atom substitution sites and in the active-center region (Table I). The former can be attributed to phasing artifacts and possible TFA alkylation at the sulfhydryl sites but does not imply any substantial increase of error elsewhere in the electron-density map. The large positive peak at the center of the active site shows clearly the position of the TFA moiety as bound to cysteine-149. The negative peak at the substrate anion-binding site (Olsen et al., 1976b) shows that the substrate analogue extends far enough to displace the sulfate anion but will not completely occupy the site, since the analogue is shorter than the true substrate.

There are three distinct features which show conformational asymmetry. The substrate peaks are noticeably elongated with the direction of elongation equivalent in Q-axis related subunits, but not between R- or P-axis related subunits. There is a negative peak between His-176 and Asn-313 which is significantly larger in the red and yellow subunits than in the blue and green subunits. Finally, a negative peak between Cys-149 and the nicotinamide ring occurs only in the green and blue subunits. In view of the apparent Q-axis symmetry of these results, the difference map was averaged about the Q molec-

TABLE I: Analysis of Peaks in the Unaveraged ($F_{TFA} - F_{holo}$) Difference Electron-Density Map.[a]

Peak	Coordinates of position in red subunit (Å)			Height (arbitrary units)			
	P	*Q*	*R*	Red	Yellow	Blue	Green
Heavy-atom A site	16.8	−14.25	8.0	635	590	530	661
Heavy-atom B site	32.4	−11.25	−6.8	290	301	354	479
TFA site	13.0	−7.50	13.0	413	489	345	456
Anion-displacement site	12.0	−5.25	16.0	−223	−332	−268	−304
Negative peak between His-176 and Asn-313	12.0	−7.50	9.0	−351	−252	−174	−183
Negative peak between Cys-149 and nicotinamide	14.0	−11.25	12.0	−38	−107	−243	−194

[a] All other peaks within a crystallographic asymmetric unit were less than 180. The root mean square density is 59 arbitrary units taken over the whole asymmetric unit.

TABLE II: Analysis of Peaks in the *Q*-Averaged ($F_{TFA} - F_{holo}$) Difference Electron-Density Map.[a]

Peak	Coordinates of position in red subunit (Å)			Height (arbitrary units)	
	P	*Q*	*R*	Red/yellow	Green/blue
Heavy-atom A site	16.8	−14.25	8.0	605	561
Heavy-atom B site	32.4	−11.25	−6.8	284	382
TFA site	13.0	−7.50	13.0	438	388
Anion-displacement site	12.0	−5.25	16.0	−270	−286
Negative peak between His-176 and Asn-313	12.0	−7.50	9.0	−253	−174
Negative peak between Cys-149 and nicotinamide	14.0	−11.25	12.0	−72	−219

[a] All other peaks within the molecular envelope were less than 170.

TABLE III: Analysis of Peaks in Difference-Difference Maps of ($F_{TFA} - F_{holo}$) Electron Density.

TFA[a] substrate site	Height (in arbitrary units)		
	Q av	*P* av	*R* av
A	330	35	105
B	120	12	45
C	−130	41	−57
D	−224	28	−41

[a] See Figure 6 for significance of A, B, C, D nomenclature.

FIGURE 3: Comparison of the *Q*-averaged ($F_{TFA} - F_{holo}$) difference electron-density map through the active-center region for (a) the red/yellow subunit and (b) the green/blue subunit. Note the different direction of elongation of the TFA peak in the two subunits.

ular diad (Figure 3). The significance of the peaks on the resultant averaged map is analyzed in Table II and shown in Figures 4 and 5. The features associated with the TFA substrate analogue, the substrate anion-binding site, the His-Asn peak in the red and yellow subunits, and the cysteine-nicotinamide peak in the green and blue subunits are seen to be well above noise level. The asymmetry of the features in the active-center regions cannot be attributed to a systematic error in the sampling of the reciprocal lattice, since (1) the features at the heavy-atom sites are spherically symmetric and (2) the asymmetry of the GAPDH molecule obeys the molecular *Q* axis but not the crystallographic symmetry.

In order to discern the significance of the asymmetry in the *Q*-averaged map, a difference-difference map was computed between the difference density in the red/yellow subunit ($\Delta\rho_R + \Delta\rho_Y$) and the difference density in the green/blue subunit ($\Delta\rho_G + \Delta\rho_B$). Thus, the difference-difference map represents the function ($\Delta\rho_R + \Delta\rho_Y - \Delta\rho_G - \Delta\rho_B$). Figure 6 shows the predicted overlap and corresponding distribution of positive and negative density. The two positive peaks in this theoretical difference map have been named A and B, while the two negative peaks are termed C and D. If the asymmetry is significant, then these peaks should stand out above the background on the difference-difference map, as is indeed shown in Table III. In order to demonstrate that the unaveraged map is symmetrical about the *Q* axis, but not about the *P* or *R* axis, similar calculations were performed for *P* ($\Delta\rho_R + \Delta\rho_G - \Delta\rho_Y - \Delta\rho_B$) and *R* ($\Delta\rho_R + \Delta\rho_B - \Delta\rho_Y - \Delta\rho_G$) axes difference-difference maps (Table III). These maps had no outstanding peaks in the active-center region or anywhere else, showing that the asymmetric effect is averaged out in these two cases.

Discussion

The demonstration of asymmetry in the crystalline GAPDH-TFA tetrameric complex shows that the molecule

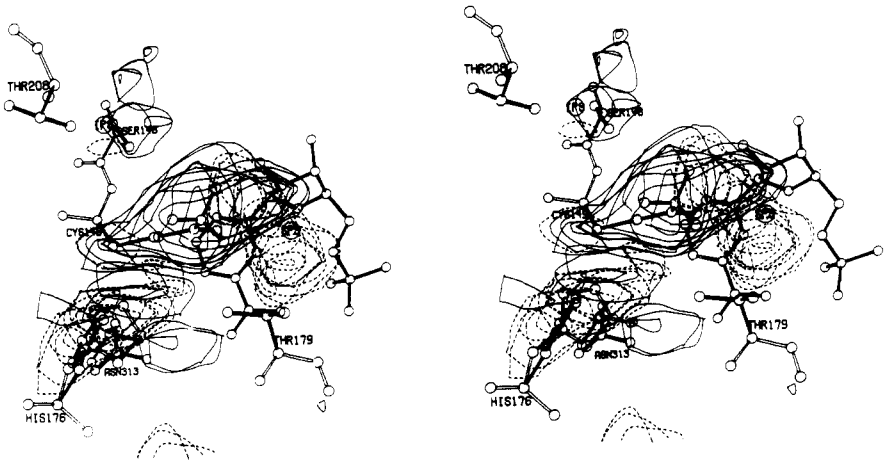

FIGURE 4: Stereo plot of the red/yellow subunit difference density with the active-site residues (black bonds) as proposed for the green/blue subunit (Moras et al., 1975) superimposed. Shown also are the sites of the sulfate anion positions at the substrate site (SPS), the inorganic phosphate sites (IPS), the proposed position (open bonds) of His-176 in the red/yellow subunit of the TFA complex, and the TFA adduct.

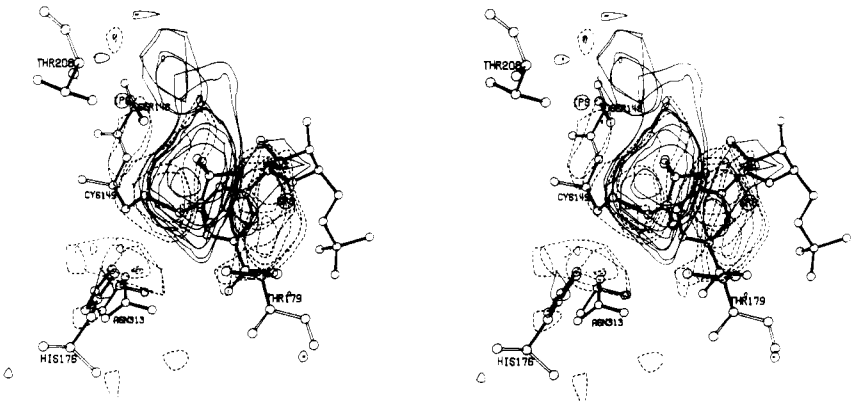

FIGURE 5: The same as Figure 4 except that the difference electron density is that for the green/blue subunit and the TFA molecule is in a possible position which would permit reduction by NADH.

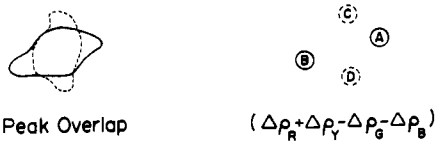

FIGURE 6: Diagrammatic representation of difference-difference density between red/yellow (continuous) and green/blue (dotted) densities. (a) Superposition of densities. (b) Subtraction of the densities in a with labeled peak areas. Orientations are shown similar to those in Figure 3.

must have been specifically oriented during crystallization. Although the detected differences occur entirely in the active center, away from the molecular surface and intermolecular contact areas, the surfaces must be asymmetric to permit such a specific molecular orientation in the crystal. In light of the absence of any detected surface structural asymmetry, it must be concluded that this property is manifested by charge differences undetectable by the present results. In contrast, molecules of GAPDH containing one NAD^+ molecule per tetramer have their subunits randomly placed within the same crystal-packing arrangement (Olsen et al., 1976a). This observation suggests that the surface of the coenzyme-depleted GAPDH tetramer is symmetric. Thus, the observed molecular asymmetry is induced by the subsequent binding of NAD^+ to the remaining subunits of the coenzyme-depleted form or by the alkylation step.

The TFA adduct was built into the Q-averaged electron density for each of the two different subunit pairs (Figures 4 and 5, Table IV) by use of a Richards optical comparator. In the "red" subunit (red − yellow averaged density), the TFA moiety (which is planar) is stretched out toward the substrate anion-binding site in a manner analogous to the anticipated substrate-binding position (Moras et al., 1975). In the "green" subunit (green − blue averaged density), however, the CF_3 group is closer to the inorganic phosphate site. The sulfate anion at the substrate-binding site has been displaced in both subunits. The positive peak in the red subunit extends close to the nicotinamide ribose, suggesting that this ring has moved toward the substrate. This is supported by a pair of negative and positive peaks in the vicinity of the pyrophosphate. In the green subunit, the nicotinamide moiety moves away from Cys-149 as shown by the negative peak between Cys-149 and the nicotinamide ring with a corresponding positive peak along the far edge of the ring. Finally, histidine-176 in the red subunit

TABLE IV: Coordinates of TFA Adduct in Angstroms.

O(1)
‖
S–C(1)H_2C(2)C(3)F_3

	Red/yellow subunit			Green/blue subunit		
	P	*Q*	*R*	*P*	*Q*	*R*
C(1)	14.4	−8.2	12.5	−13.6	8.8	12.6
C(2)	13.6	−7.6	13.6	−13.3	7.6	13.5
O(1)	12.8	−8.3	14.3	−12.5	6.7	13.1
C(3)	13.8	−6.3	14.0	−13.9	7.5	14.6

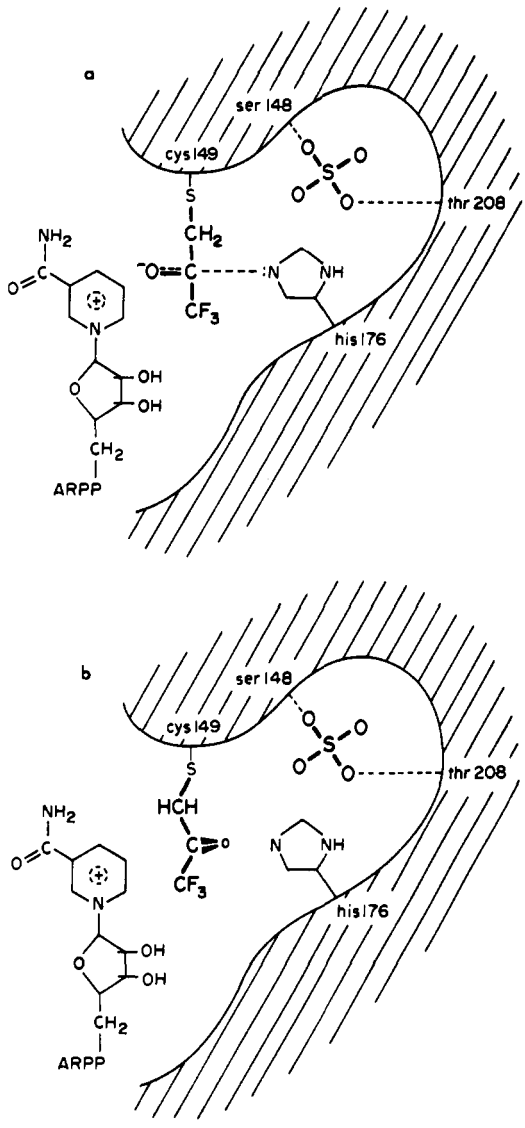

FIGURE 7: Schematic showing (a) nucleophilic attack by histidine on TFA as is suggested for the red/yellow subunit and (b) the TFA adduct oriented for reduction as might occur in the presence of NADH in the green/blue subunit.

can readily be seen to have moved toward the substrate position, whereas in the green subunit there is a suggestion that histidine-176 moves away from the substrate.

Bode et al. (1975a) concluded from their NMR results that a nucleophile interacts with the TFA carbonyl in one of the two environments (Figure 7a), leaving the other species in a conformation susceptible for reduction by NADH (Figure 7b). They also suggested that histidine-176 acted as the pH-sensitive nucleophile. The current results are consistent with their interpretation. The nucleophilic attack on the TFA carbonyl in the red subunit is made possible by the closer approach of histidine-176. The subsequent increase of negative charge on the carbonyl oxygen counteracts the positive charge on the NAD^+ in the absence of sulfate ion or substrate phosphate. The histidine attack would be negated in more acid pHs but it is not understood why the replacement of the carboxyamide with an aldehyde moiety eliminates pH sensitivity.

With the current results, it is difficult to discern the mechanism through which the molecular asymmetry is induced upon ligand binding. The abortive ternary complex and holoenzyme structures give no indication of structural alterations which would explain the appearance of asymmetric active-center conformations. Thus, it is not possible to determine whether primary conformational change occurs during NAD^+ binding or alkylation of the holoenzyme. Nevertheless, the structural asymmetry of an enzyme–substrate complex has been clearly demonstrated for GAPDH.

Acknowledgments

We are grateful for the critical comments of Drs. Kenneth W. Olsen and Daniel E. Koshland, Jr., and would like to thank Karen Babos and Sharon Wilder for help in the preparation of the manuscript.

References

Adams, M. J., McPherson, A., Jr., Rossmann, M. G., Schevitz, R. W., and Wonacott, A. J. (1970), *J. Mol. Biol. 51,* 31–38.

Allison, W. S. (1966), *Methods Enzymol. 9,* 210–215.

Anderson, W. F., and Steitz, T. A. (1975), *J. Mol. Biol. 92,* 279–287.

Bentley, G., Dodson, E., Dodson, G., Hodgkin, D., and Mercola, D. (1976), *Nature (London) 261,* 166–168.

Bernhard, S. A., and MacQuarrie, R. A. (1973), *J. Mol. Biol. 74,* 73–78.

Blundell, T., Dodson, G., Hodgkin, D., and Mercola, D. (1972), *Adv. Protein Chem. 26,* 279–402.

Bode, J., Blumenstein, M., and Raftery, M. A. (1975a), *Biochemistry 14,* 1153–1160.

Bode, J., Blumenstein, M., and Raftery, M. A. (1975b), *Biochemistry 14,* 1146–1152.

Boers, W., Oosthuizen, C., and Slater, E. C. (1971), *Biochim. Biophys. Acta 250,* 35–46.

Boers, W., and Slater, E. C. (1973), *Biochim. Biophys. Acta 315,* 272–284.

Buehner, M., Ford, G. C., Moras, D., Olsen, K. W., and Rossmann, M. G. (1974a), *J. Mol. Biol. 90,* 25–49.

Buehner, M., Ford, G. C., Moras, D., Olsen, K. W., and Rossmann, M. G. (1974b), *J. Mol. Biol. 82,* 563–585.

Champness, J. N., Bloomer, A. C., Bricogne, G., Butler, P. J. G., and Klug, A. (1976), *Nature (London) 259,* 20–24.

Conway, A., and Koshland, D. E., Jr. (1968), *Biochemistry 7,* 4011–4023.

Cook, R. A., and Koshland, D. E., Jr. (1970), *Biochemistry 9,* 3337–3342.

De Vijlder, J. J. M., Boers, W., and Slater, E. C. (1969), *Biochim. Biophys. Acta 191,* 214–220.

Drenth, J., Kalk, K. H., and Swen, H. M. (1976), *Biochemistry 15,* 3731–3738.

Hill, E., Tsernoglou, D., Webb, L., and Banaszak, L. J. (1972), *J. Mol. Biol. 72,* 577–591.

Hodgkin, D. C. (1974), *Proc. R. Soc. London, Ser. B 186,* 191–215.

Jack, A., Weinzierl, J., and Kalb, A. J. (1971), *J. Mol. Biol. 58,* 389–395.

Kirschner, K. (1971), *J. Mol. Biol. 58,* 51–68.

Kirschner, K., Gallego, E., Schuster, I., and Goodall, D. (1971), *J. Mol. Biol. 58,* 29–50.

Krimsky, I., and Racker, E. (1955), *Science 122,* 319–321.

Levitzki, A. (1973), *Biochem. Biophys. Res. Commun. 54,* 889–893.

MacQuarrie, R. A., and Bernhard, S. A. (1971), *J. Mol. Biol. 55,* 181–192.

McCaul, S., and Byers, L. D. (1976), *Biochem. Biophys. Res. Commun. 72,* 1028–1034.

Mercer, W. D., Winn, S. I., and Watson, H. C. (1976), *J. Mol. Biol. 104,* 277–283.

Moras, D., Olsen, K. W., Sabesan, M. N., Buehner, M., Ford, G. C., and Rossmann, M. G. (1975), *J. Biol. Chem. 150,* 9137-9162.
Olsen, K. W., Garavito, R. M., Sabensan, M. N., and Rossmann, M. G. (1976a), *J. Mol. Biol. 107,* 577-584.
Olsen, K. W., Garavito, R. M., Sabesan, M. N., and Rossmann, M. G. (1976b), *J. Mol. Biol. 107,* 571-576.
Racker, E., and Krimsky, I. (1952), *J. Biol. Chem. 198,* 731-743.
Robertus, J. D., Alden, R. A., Birktoft, J. J., Kraut, J., Powers, J. C., and Wilcox, P. E. (1972), *Biochemistry 11,* 2439-2449.
Schlessinger, J., and Levitzki, A. (1974), *J. Mol. Biol. 82,* 547-561.
Segal, D. M., Powers, J. C., Cohen, G. H., Davies, D. R., and Wilcox, P. E. (1971), *Biochemistry 10,* 3728-3738.
Seydoux, F., Bernhard, S., Pfenninger, O., Payne, M., and Malhotra, O. P. (1973), *Biochemistry 12,* 4290-4300.
Seydoux, F. J., Kelemen, N., Kellershohn, N., and Roucous, C. (1976), *Eur. J. Biochem. 64,* 481-489.
Stallcup, W. B., and Koshland, D. E., Jr. (1973), *J. Mol. Biol. 80,* 41-62.
Tulinsky, A., Vandlen, R. L., Morimoto, C. N., Mani, N. V., and Wright, L. H. (1973), *Biochemistry 12,* 4185-4192.
Watson, H. C., and Banaszak, L. J. (1964), *Nature (London) 204,* 918-920.
Watson, H. C., Duée, E., and Mercer, W. D. (1972), *Nature (London) New Biol. 240,* 130-133.

Distribution of Alkali Light Chains in Myosin: Isolation of Isoenzymes†

John C. Holt‡ and Susan Lowey*

ABSTRACT: Antibodies have been isolated which are specific for the "difference peptide" unique to the alkali 1 light chain (mol wt 20 700) of chicken breast muscle myosin. When coupled to Sepharose as an immunoadsorbent, they are capable of resolving subfragment 1, heavy meromyosin, and myosin into two fractions, one rich in alkali 1 and the other rich in alkali 2. This fractionation provides direct evidence for the existence of two isoenzymic populations in vertebrate skeletal myosin. The ability of antibodies to the difference peptide to distinguish between alkali 1 and 2 provides a marker which will allow the distribution of alkali light chains in muscle fibers and filaments to be investigated.

The low molecular weight subunits of vertebrate skeletal myosin fall into two classes: DTNB light chains (2 mol/mol of myosin), which can be selectively dissociated by the thiol reagent DTNB,[1] and alkali 1 and 2 light chains (a total of 2 mol/mol of myosin), which are released only under denaturing conditions such as exposure to pH 11 (Weeds, 1969; Gazith et al., 1970; Weeds and Lowey, 1971). The two species of alkali light chains are closely related, although clearly the products of different genes (Weeds and Frank, 1972). The sequence of alkali 2 (mol wt 16 500) is repeated in alkali 1 (mol wt 20 700) with only five substitutions. The unique feature of alkali 1 is an N-terminal sequence of 41 residues which accounts for its higher molecular weight (Frank and Weeds, 1974). This sequence, which is rich in proline, alanine, and lysine, is termed the "difference peptide".

There are two distinct ways in which the closely related alkali 1 and 2 subunits may be distributed in myosin. Either a single type of myosin molecule exists, in which the two heads differ with respect to their alkali l.c. (heterodimers) or, alternatively, there may be two isoenzymic forms of myosin with the two heads of each molecule containing the same light chain (homodimers). A third possibility which must be recognized is the occurrence of a mixture of homodimers and heterodimers.

The isoenzyme interpretation has received some indirect support from observations on the stoichiometry of alkali l.c. in rabbit skeletal myosin. The light chains have been found to occur in the proportions 1.2-1.4 mol of alkali 1 to 2 mol of DTNB l.c. to 0.6-0.8 mol of alkali 2 (Lowey and Risby, 1971; Sarkar, 1972; Weeds et al., 1975). The unequal amounts of alkali 1 and 2 have been taken to imply that the myosin contains unequal amounts of two homodimers, rather than a uniform population of heterodimers. Since both alkali l.c. were found not only in mixed back and leg muscles but also in single fibers taken from a more histochemically homogeneous region of the psoas (Weeds et al., 1975), the isoenzymes cannot arise simply from the mixing of different fiber types. It must be pointed out, however, that in myosin from chicken breast muscle the amounts of alkali 1 and 2 are essentially equal (Lowey and Risby, 1971), so that the existence of homodimers is not necessarily to be inferred.

A more direct approach to the distribution of the alkali l.c. in a myosin preparation is to fractionate the presumed isoenzymes. So far this has been achieved for S1, the single head of myosin, which can be resolved into alkali 1 and 2 types by chromatography on DEAE-cellulose (Yagi and Otani, 1974; Weeds and Taylor, 1975). Information on the composition of intact myosin must come, however, from the fractionation of

† From the Rosenstiel Basic Medical Sciences Research Center and the Graduate Department of Biochemistry, Brandeis University, Waltham, Massachusetts 02154. *Received March 28, 1977.* This work was supported by grants from the National Science Foundation (PCM 75-14790), the National Institute of Arthritis, Metabolism and Digestive Diseases, U.S. Public Health Service (AM 17350), and the Muscular Dystrophy Association, Inc.

‡ Present address: National Institute for Biological Standards and Control, London NW3 6RB, U.K.

[1] Abbreviations used are: DTNB, 5,5′-dithiobis(2-nitrobenzoic acid); HMM, heavy meromyosin; S1, subfragment 1; EDTA, ethylenediaminetetraacetic acid; Gdn·HCl, guanidine hydrochloride; DEAE, diethylaminoethyl.